

## Synthesis of $\text{Ce}_2\text{Rh}_3\text{Ge}_5$ Crystals from a Bismuth Flux

Daniel Voßwinkel and Rainer Pöttgen

Institut für Anorganische und Analytische Chemie,  
Universität Münster, Corrensstrasse 30, D-48149  
Münster, Germany

Reprint requests to R. Pöttgen.

E-mail: [pottgen@uni-muenster.de](mailto:pottgen@uni-muenster.de)

*Z. Naturforsch.* **2013**, 68b, 301–305

DOI: 10.5560/ZNB.2013-3015

Received January 17, 2013

The germanide  $\text{Ce}_2\text{Rh}_3\text{Ge}_5$  was synthesized from the elements in a bismuth flux, and the structure was refined from single-crystal X-ray diffractometer data:  $\text{U}_2\text{Co}_3\text{Si}_5$  type, *Ibam*,  $a = 1010.1(2)$ ,  $b = 1210.4(2)$ ,  $c = 599.1(1)$  pm,  $wR = 0.0596$ , 760 structure factors, 31 variables. The rhodium and germanium atoms build up a three-dimensional  $[\text{Rh}_3\text{Ge}_5]$  network (242–269 pm Rh–Ge; 300 pm Rh–Rh; 266 pm Ge–Ge) in which the cerium atoms fill cavities. Each cerium atom has coordination number 17 by ten germanium (302–331 pm) and seven rhodium (320–355 pm) neighbors. The crystal-chemical relation of the  $\text{Ce}_2\text{Rh}_3\text{Ge}_5$  ( $\equiv \text{CeRh}_{1.5}\text{Ge}_{2.5}$ ) structure with that of  $\text{CeRh}_2\text{Ge}_2$  ( $\text{ThCr}_2\text{Si}_2$  type) is discussed.

**Key words:** Cerium, Intermetallics, Crystal Chemistry,  
Crystal Growth

### Introduction

Single crystals of intermetallic compounds can be grown in different dimensions. Usually the Czochralski or Bridgman techniques are used for crystals in mm or even cm size for orientation-dependent physical property measurements. Such experiments are expensive, material- and time-consuming and mostly conducted only for selected compounds with interesting physical properties.

For explorative synthesis and the growth of small crystals ( $\mu\text{m}$  to mm scale) for structure determination, flux-assisted synthesis is an effective tool. Besides eutectic salt fluxes [1, 2], also a variety of low-melting metal fluxes has been utilized [3, 4]. The broad applicability of metal fluxes for different classes of intermetallics has recently been summarized in a special issue of *Philosophical Magazine B* devoted to the growth of novel materials [5–11].

Crystals of metal germanides were often grown from aluminum and gallium fluxes; however, in many cases aluminum and gallium act as a reactive flux, and one observes substantial incorporation into the structure. Several examples are summarized in [4]. Indium on the other hand seems to be a good candidate for a non-reactive flux, as recently shown for the synthesis of  $\text{DyNiGe}_2$  [12],  $\text{Eu}_2\text{AuGe}_3$  [13] and  $\text{Yb}_5\text{Ni}_4\text{Ge}_{10}$  [14] crystals. Good results have also been obtained with bismuth fluxes for the phosphides  $\text{RERh}_6\text{P}_4$  ( $\text{RE} = \text{Sc}, \text{Yb}, \text{Lu}$ ) [15], and this has been applied to the germanide  $\text{CeRh}_6\text{Ge}_4$  [16]. In continuation of the bismuth flux crystal growth experiments of germanides we have now obtained well-shaped crystals of  $\text{Ce}_2\text{Rh}_3\text{Ge}_5$  with  $\text{U}_2\text{Co}_3\text{Si}_5$ -type structure. So far  $\text{Ce}_2\text{Rh}_3\text{Ge}_5$  has only been characterized by its lattice parameters based on powder X-ray data [17–21]. The flux growth conditions and single-crystal diffraction data are reported herein.

### Experimental

#### Synthesis

The  $\text{Ce}_2\text{Rh}_3\text{Ge}_5$  sample was synthesized from the elements in a bismuth flux, similar to  $\text{CeRh}_6\text{Ge}_4$  [16]. Starting materials were sublimed cerium pieces (Johnson Matthey), rhodium powder (Heraeus), germanium pieces (Chempur), and elongated bismuth shots (ABCR), all with stated purities better than 99.9%. The elements were weighed in the atomic ratio Ce:Rh:Ge:Bi of 2:1:2:25 and sealed in an evacuated silica ampoule. The latter was placed in a muffle furnace, heated to 1320 K within 2 h, kept at that temperature for 1 h, then cooled to 570 K at a rate of 8 K/h and finally to 530 K at a rate of 2 K/h. The furnace was then switched off and the ampoule cooled to room temperature by radiative heat loss. The excess flux was dissolved in a 1:1 molar mixture of  $\text{H}_2\text{O}_2$  (ACROS, 35%) and glacial acetic acid (VWR International) at 373 K. The resulting crystals were washed with deionized water.  $\text{Ce}_2\text{Rh}_3\text{Ge}_5$  is stable in air over months.

#### X-Ray diffraction

Parts of the crystalline  $\text{Ce}_2\text{Rh}_3\text{Ge}_5$  sample were ground to a fine powder in an agate mortar and characterized by a Guinier powder pattern (Guinier camera, Fuji-film image plate system, BAS-1800 read-out system) using  $\text{Cu } K_{\alpha 1}$  radiation and  $\alpha$ -quartz ( $a = 491.30$ ,  $c = 540.46$  pm) as an internal standard. The orthorhombic lattice parameters (Table 1)

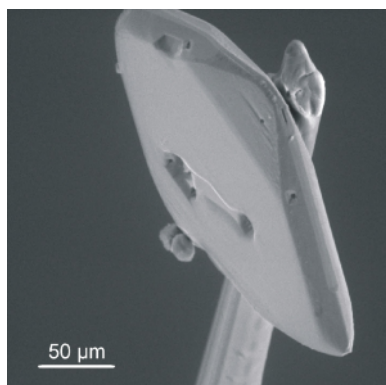


Fig. 1. A single crystal of  $\text{Ce}_2\text{Rh}_3\text{Ge}_5$  mounted on a quartz fiber.

were obtained from a least-squares refinement of the powder data. Correct indexing was ensured through an intensity calculation [22].

Well-shaped single crystals of  $\text{Ce}_2\text{Rh}_3\text{Ge}_5$  (a selected platelet is shown in Fig. 1) were selected from the flux-grown sample and glued to thin quartz fibers. Their quality was checked by Laue photographs on a Buerger camera (white Mo radiation). Intensity data were collected at room temperature by use of a Stoe Stadi Vari diffractometer equipped with a Mo micro focus source and a Pilatus detection system and scaled subsequently according to the Gaussian-shaped profile of the X-ray source. A numerical absorption correction was applied to the data set. All relevant details concerning the data collection and evaluation are listed in Table 2.

#### EDX data

Semiquantitative EDX analyses of the single crystal studied on the diffractometer were carried out in variable pressure mode with a Zeiss EVO<sup>®</sup> MA10 scanning electron microscope with  $\text{CeO}_2$ , Rh, and Ge as standards. The experimentally observed average composition was close to the ideal one. No impurity elements (especially no residual bismuth from the flux) were detected.

## Results and Discussion

#### Structure refinement

The isotypy of  $\text{Ce}_2\text{Rh}_3\text{Ge}_5$  with the orthorhombic  $\text{U}_2\text{Co}_3\text{Si}_5$  type [23] was already evident from the Guinier powder pattern. Careful examination of the data set revealed a body-centered orthorhombic lattice, and the systematic extinctions were compatible with space group *Ibam*. The atomic parameters of the crystal-chemically closely related phase

Table 1. Lattice parameters of  $\text{Ce}_2\text{Rh}_3\text{Ge}_5$ .

<i>a</i> (pm)	<i>b</i> (pm)	<i>c</i> (pm)	<i>V</i> (nm <sup>3</sup> )	Reference
1010.1(2)	1210.4(2)	599.1(1)	0.7325	this work
1009	1209	605.6	0.7388	[20]
1010	1211.1	599.8	0.7337	[19]
1009.7(6)	1209(1)	598.7(5)	0.7308	[17]

Table 2. Crystal data and structure refinement for  $\text{Ce}_2\text{Rh}_3\text{Ge}_5$ .

Empirical formula	$\text{Ce}_2\text{Rh}_3\text{Ge}_5$
Formula weight, g mol <sup>-1</sup>	951.9
Lattice parameters (Guinier powder data)	
<i>a</i> , pm	1010.1(2)
<i>b</i> , pm	1210.4(2)
<i>c</i> , pm	599.1(1)
Cell volume <i>V</i> , nm <sup>3</sup>	0.7325
Space group; <i>Z</i>	<i>Ibam</i> ; 4
Structure type; Pearson code	$\text{U}_2\text{Co}_3\text{Si}_5$ ; oI40
Calculated density, g cm <sup>-3</sup>	8.63
Crystal size, μm <sup>3</sup>	30 × 170 × 170
Transmission ratio (min / max)	0.815 / 0.904
Absorption coefficient, mm <sup>-1</sup>	38.8
<i>F</i> (000), e	1644
θ range for data collection, deg	2–34
Range in <i>hkl</i>	±15, ±17, ±9
Total no. of reflections	5018
Independent reflections / <i>R</i> <sub>int</sub>	760 / 0.0568
Reflections with <i>I</i> > 2σ( <i>I</i> ) / <i>R</i> <sub>σ</sub>	582 / 0.0626
Data / parameters	760 / 31
Goodness-of-fit on <i>F</i> <sup>2</sup>	0.850
<i>R</i> 1 / <i>wR</i> 2 for <i>I</i> > 2σ( <i>I</i> )	0.0275 / 0.0602
<i>R</i> 1 / <i>wR</i> 2 for all data	0.0327 / 0.0596
Extinction coefficient	0.0275(8)
Largest diff. peak / hole, e Å <sup>-3</sup>	2.19 / -2.74

$\text{Ce}_2\text{Rh}_3\text{Si}_5$  [24] were taken as starting values, and the structure was refined with anisotropic displacement parameters for all atoms with SHELXL-97 (full-matrix least-squares on *F*<sub>o</sub><sup>2</sup>) [25, 26]. In a separate refinement of the occupancy parameters no deviation from the ideal composition was observed. A final difference Fourier synthesis showed no significant residual peaks. The refined atomic positions, the displacement parameters and the interatomic distances are given in Tables 3–5.

Further details of the crystal structure investigation may be obtained from Fachinformationszentrum Karlsruhe, 76344 Eggenstein-Leopoldshafen, Germany (fax: +49-7247-808-666; E-mail: [crysdata@fiz-karlsruhe.de](mailto:crysdata@fiz-karlsruhe.de), [http://www.fiz-karlsruhe.de/request\\_for\\_deposited\\_data.html](http://www.fiz-karlsruhe.de/request_for_deposited_data.html)) on quoting the deposition number CSD-425650.

Table 3. Atomic coordinates and equivalent isotropic displacement parameters ( $\text{pm}^2$ ) for  $\text{Ce}_2\text{Rh}_3\text{Ge}_5$ .  $U_{\text{eq}}$  is defined as one third of the trace of the orthogonalized  $U_{ij}$  tensor.

Atom	Site	$x$	$y$	$z$	$U_{\text{eq}}$
Ce	8j	0.26804(6)	0.36669(4)	0	140(2)
Rh1	8j	0.10502(9)	0.14053(6)	0	151(2)
Rh2	4b	1/2	0	1/4	144(2)
Ge1	8j	0.33944(12)	0.09953(8)	0	146(2)
Ge2	8g	0	0.27801(9)	1/4	152(2)
Ge3	4a	0	0	1/4	152(3)

Table 4. Anisotropic displacement parameters ( $\text{pm}^2$ ) for  $\text{Ce}_2\text{Rh}_3\text{Ge}_5$ .  $U_{23} = 0$

Atom	$U_{11}$	$U_{22}$	$U_{33}$	$U_{12}$	$U_{13}$
Ce	149(3)	144(3)	126(2)	−4(2)	0
Rh1	153(4)	140(3)	160(3)	2(3)	0
Rh2	155(5)	158(5)	119(4)	0	0
Ge1	156(5)	149(5)	134(4)	10(4)	0
Ge2	163(6)	166(5)	126(4)	0	10(4)
Ge3	168(8)	165(6)	124(5)	0	0

Table 5. Interatomic distances (pm) for  $\text{Ce}_2\text{Rh}_3\text{Ge}_5$  calculated with the powder lattice parameters. Standard deviations are equal or smaller than 0.1 pm. All distances of the first coordination spheres are listed.

Ce:	1	Ge1	302.0	Rh2:	4	Ge1	251.5
	1	Rh1	319.5		2	Ge2	268.7
	2	Ge1	321.2		2	Rh2	299.6
	2	Ge3	321.5		4	Ce	349.0
	2	Rh1	326.0	Ge1:	1	Rh1	241.9
	2	Ge2	327.5		2	Rh2	251.5
	2	Ge2	328.6		2	Ge2	265.9
	1	Ge1	331.3		1	Ce	302.0
	1	Rh1	340.5		2	Ce	321.2
	2	Rh2	349.0		1	Ce	331.3
Rh1:	1	Rh1	355.4	Ge2:	2	Rh1	247.7
	1	Ge1	241.9		2	Ge1	265.9
	2	Ge2	247.7		1	Rh2	268.7
	2	Ge3	250.2		2	Ge2	299.6
	1	Ce	319.5	Ge3:	2	Ce	327.5
	2	Ce	326.0		2	Ce	328.7
	1	Ce	340.5		4	Rh1	250.2
	1	Ce	355.4		2	Ge3	299.6
					4	Ce	321.5

### Crystal chemistry

Well-shaped platelet-like single crystals of  $\text{Ce}_2\text{Rh}_3\text{Ge}_5$  were obtained from a bismuth flux, and the  $\text{Ce}_2\text{Rh}_3\text{Ge}_5$  structure was refined from single-crystal diffraction data.  $\text{Ce}_2\text{Rh}_3\text{Ge}_5$  crystals have two crystallographically independent rhodium and three such germanium sites. The unit cell and

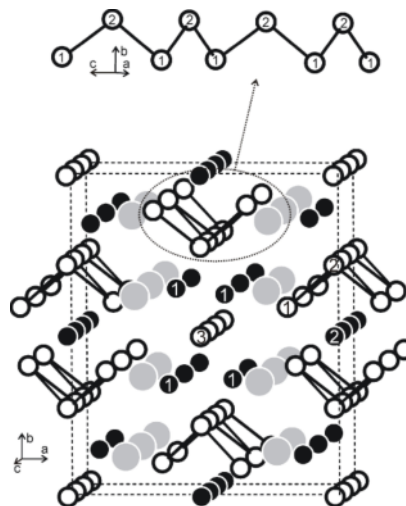


Fig. 2. The crystal structure of  $\text{Ce}_2\text{Rh}_3\text{Ge}_5$ . Cerium, rhodium and germanium atoms are drawn as medium grey, black filled and open circles, respectively. The germanium substructure is emphasized. The crystallographically independent rhodium and germanium atoms are indicated.

the germanium substructure are presented in Fig. 2. The Ge3 atoms have no nearest germanium neighbors and can, to a first approximation, be considered as  $\text{Ge}^{4-}$  germanide anions. The Ge1 and Ge2 atoms build up infinite  $-\text{Ge1}-\text{Ge2}-\text{Ge1}-\text{Ge2}-$  zig-zag chains with 266 pm Ge1–Ge2 distance, slightly longer than the Ge–Ge distance of 245 pm in the element [27]. If we compare these zig-zag chains with those in CrB-type PrGe (264 pm) [28] and SrGe (262 pm) [29] or EuIrGe<sub>2</sub> (257 pm) [30], one can ascribe to it single bond character and a formal charge of  $\text{Ge}^{2-}$  (chalcogen electron configuration).

Together, the rhodium and germanium atoms build up a complex three-dimensional  $[\text{Rh}_3\text{Ge}_5]$  polyanionic network (Fig. 3) with Rh–Ge distances ranging from 242 to 269 pm, in good agreement with the sum of the covalent radii [31] of 247 pm. Comparable ranges have been observed in CeRhGe (251–261 pm) [32],  $\text{CeRh}_2\text{Ge}_2$  (246 pm) and  $\text{CeRh}_6\text{Ge}_4$  (247–255 pm) [16]. The stability of all these polyanions is mainly governed by strong covalent Rh–Ge bonding. The slightly larger germanium content in  $\text{Ce}_2\text{Rh}_3\text{Ge}_5$  leads to additional Ge–Ge bonds (*vide ultra*). The shortest Rh–Rh distance of 300 pm is much longer than in *fcc* rhodium (269 pm) [27], and one can only ascribe weakly bonding character to these contacts.

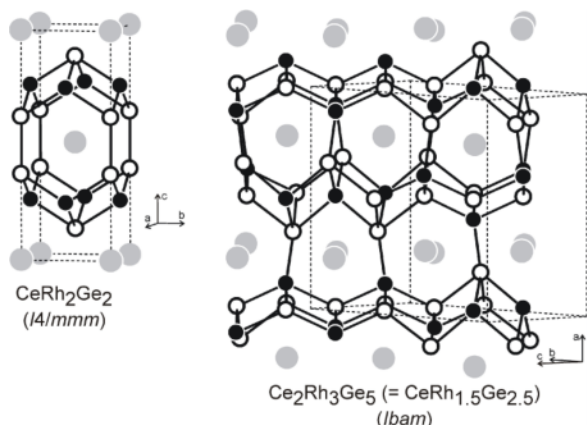


Fig. 3. The crystal structures of  $\text{CeRh}_2\text{Ge}_2$  and  $\text{Ce}_2\text{Rh}_3\text{Ge}_5$ . Cerium, rhodium and germanium atoms are drawn as medium grey, black filled and open circles, respectively. The three-dimensional  $[\text{Rh}_2\text{Ge}_2]$  and  $[\text{Rh}_3\text{Ge}_5]$  polyanionic networks are emphasized.

The cerium atoms are coordinated by 10 Ge + 7 Rh atoms (Fig. 3). The large cavity around the

cerium atoms reminds of the structure of tetragonal  $\text{CeRh}_2\text{Ge}_2$  [16]. Both structures derive from the arsitotype  $\text{BaAl}_4$  [33]. In  $\text{CeRh}_2\text{Ge}_2$ , the cerium coordination is much more symmetric. The cerium atoms have site symmetry  $4/mmm$  and coordination number 18 by ten germanium and eight rhodium atoms. In going to  $\text{Ce}_2\text{Rh}_3\text{Ge}_5$  ( $\equiv \text{CeRh}_{1.5}\text{Ge}_{2.5}$ ) the rhodium-to-germanium ratio changes, leading to significant distortions in the cerium coordination, and the cerium site symmetry is reduced to  $.m$ . A major difference between the cerium coordination in  $\text{CeRh}_2\text{Ge}_2$  and  $\text{Ce}_2\text{Rh}_3\text{Ge}_5$  concerns the Ce–Rh distances:  $8 \times 335$  pm in  $\text{CeRh}_2\text{Ge}_2$  vs.  $320$  ( $1 \times$ ),  $326$  ( $2 \times$ ),  $341$  ( $1 \times$ ),  $349$  ( $2 \times$ ), and  $355$  ( $1 \times$ ) pm in  $\text{Ce}_2\text{Rh}_3\text{Ge}_5$ . In order to preserve Ce–Rh bonding, three shorter Ce–Rh bonds occur in  $\text{Ce}_2\text{Rh}_3\text{Ge}_5$  as compared to  $\text{CeRh}_2\text{Ge}_2$ .

#### Acknowledgement

We thank Dipl.-Ing. U. Ch. Rodewald and Dr. R.-D. Hoffmann for the intensity data collection. This work was financially supported by the Deutsche Forschungsgemeinschaft.

- [1] G. Brauer, *Handbuch der Präparativen Anorganischen Chemie*, 3. Band, 4. Abschnitt, 3. Aufl., Enke, Stuttgart, **1975**.
- [2] W. Sundermeyer, *Angew. Chem.* **1964**, 77, 241.
- [3] P. C. Canfield, Z. Fisk, *Philos. Mag. B* **1992**, 6, 1117.
- [4] M. G. Kanatzidis, R. Pöttgen, W. Jeitschko, *Angew. Chem. Int. Ed.* **2005**, 44, 6996.
- [5] G. W. Morrison, M. C. Menard, L. J. Treadwell, N. Haldolaarachchige, K. C. Kendrick, D. P. Young, J. Y. Chang, *Philos. Mag. B* **2012**, 92, 2524.
- [6] C. Krellner, S. Taube, T. Westerkamp, Z. Hossain, C. Geibel, *Philos. Mag. B* **2012**, 92, 2508.
- [7] R. A. Ribeiro, M. A. Avila, *Philos. Mag. B* **2012**, 92, 2492.
- [8] E. D. Bauer, P. H. Tobash, J. N. Mitchell, J. L. Sarrao, *Philos. Mag. B* **2012**, 92, 2466.
- [9] I. R. Fisher, M. C. Shapiro, J. G. Analytis, *Philos. Mag. B* **2012**, 92, 2401.
- [10] T. Wolf, *Philos. Mag. B* **2012**, 92, 2458.
- [11] C. Petrovic, P. C. Canfield, J. Y. Mellen, *Philos. Mag. B* **2012**, 92, 2448.
- [12] J. R. Salvador, J. R. Gour, D. Bile, S. D. Mahanti, M. G. Kanatzidis, *Inorg. Chem.* **2004**, 43, 1403.
- [13] C. P. Sebastian, C. D. Malliakas, M. Chondroudi, I. Schellenberg, S. Rayaprol, R.-D. Hoffmann, R. Pöttgen, M. G. Kanatzidis, *Inorg. Chem.* **2010**, 49, 9574.
- [14] S. C. Peter, S. Rayaprol, M. C. Francisco, M. G. Kanatzidis, *Eur. J. Inorg. Chem.* **2011**, 3963.
- [15] U. Pfannenschmidt, U. Ch. Rodewald, R. Pöttgen, *Monatsh. Chem.* **2011**, 142, 219.
- [16] D. Voßwinkel, O. Niehaus, U. Ch. Rodewald, R. Pöttgen, *Z. Naturforsch.* **2012**, 67b, 1241.
- [17] G. Venturini, M. Méot-Meyer, J. F. Maréché, B. Malaman, B. Roques, *Mater. Res. Bull.* **1986**, 21, 33.
- [18] K. Uemo, T. Takabatake, T. Suzuki, S. Hane, H. Mitamura, T. Goto, *Phys. Rev. B* **2001**, 64, 144412.
- [19] Z. Hossain, H. Ohmoto, K. Uemo, F. Iga, T. Suzuki, T. Takabatake, N. Takamoto, K. Kindo, *Phys. Rev. B* **1999**, 60, 10383.
- [20] C. Godart, C. V. Tomy, L. C. Gupta, R. Vijayaraghavan, *Solid State Commun.* **1988**, 67, 677.
- [21] K. Uemo, T. Takabatake, S. Hane, H. Mitamura, T. Goto, *Physica C* **2002**, 312–313, 403.
- [22] K. Yvon, W. Jeitschko, E. Parthé, *J. Appl. Crystallogr.* **1977**, 10, 73.
- [23] L. G. Akselrud, Yu. P. Yarmolyuk, E. I. Gladyshevskii, *Sov. Phys. Crystallogr.* **1977**, 22, 492.
- [24] A. Lipatov, A. Gribanov, A. Grytsiv, S. Safronov, P. Rogl, J. Rousnyak, Yu. Seropegin, G. Giester, *J. Solid State Chem.* **2010**, 183, 829.
- [25] G. M. Sheldrick, SHELXL-97, Program for the Refinement of Crystal Structures, University of Göttingen, Göttingen (Germany) **1997**.

- [26] G. M. Sheldrick, *Acta Crystallogr.* **2008**, A64, 112.
- [27] J. Donohue, *The Structures of the Elements*, Wiley, New York (U. S. A.) **1974**.
- [28] A. G. Tharp, G. S. Smith, Q. Johnson, *Acta Crystallogr.* **1966**, 20, 583.
- [29] W. Rieger, E. Parthé, *Acta Crystallogr.* **1967**, 22, 919.
- [30] R. Pöttgen, A. Simon, *Z. Anorg. Allg. Chem.* **1996**, 622, 779.
- [31] J. Emsley, *The Elements*, Oxford University Press, Oxford **1999**.
- [32] E. Gaudin, B. Chevalier, B. Heying, U. Ch. Rodewald, R. Pöttgen, *Chem. Mater.* **2005**, 17, 2693.
- [33] D. Kußmann, R. Pöttgen, U. Ch. Rodewald, C. Rosenhahn, B. D. Mosel, G. Kotzyba, B. Künnen, *Z. Naturforsch.* **1999**, 54b, 1155.